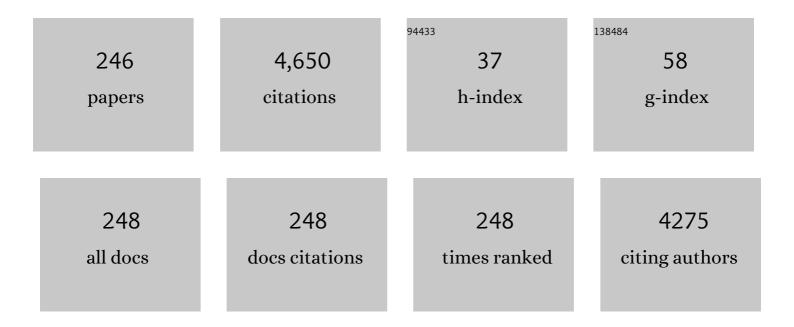
Andreas Markwitz

List of Publications by Year in descending order

Source: https://exaly.com/author-pdf/6340517/publications.pdf Version: 2024-02-01



#	Article	IF	CITATIONS
1	UV and humidity sensing properties of ZnO nanorods prepared by the arc discharge method. Nanotechnology, 2009, 20, 245502.	2.6	231
2	Controlling preferred orientation and electrical conductivity of zinc oxide thin films by post growth annealing treatment. Applied Surface Science, 2016, 367, 52-58.	6.1	229
3	Urban air quality in the Asian region. Science of the Total Environment, 2008, 404, 103-112.	8.0	160
4	Air pollution by fine particulate matter in Bangladesh. Atmospheric Pollution Research, 2013, 4, 75-86.	3.8	125
5	Precipitation, ripening and chemical effects during annealing of Ge+ implanted SiO2 layers. Nuclear Instruments & Methods in Physics Research B, 1999, 148, 969-974.	1.4	115
6	Multimodal impurity redistribution and nanocluster formation in Ge implanted silicon dioxide films. Applied Physics Letters, 1997, 71, 3215-3217.	3.3	94
7	Identification of Sources of Fine and Coarse Particulate Matter in Dhaka, Bangladesh. Aerosol and Air Quality Research, 2010, 10, 345-353.	2.1	93
8	Chemical Characterization and Source Identification of Particulate Matter at an Urban Site of Navi Mumbai, India. Aerosol and Air Quality Research, 2011, 11, 560-569.	2.1	91
9	Exploring the Variation between EC and BC in a Variety of Locations. Aerosol and Air Quality Research, 2012, 12, 1-7.	2.1	78
10	Structural and photoluminescence properties of Gd implanted ZnO single crystals. Journal of Applied Physics, 2011, 110, .	2.5	76
11	Air particulate matter pollution in Ulaanbaatar, Mongolia: determination of composition, source contributions and source locations. Atmospheric Pollution Research, 2011, 2, 126-137.	3.8	76
12	Size-controlled synthesis and gas sensing application of tungsten oxide nanostructures produced by arc discharge. Nanotechnology, 2011, 22, 335702.	2.6	73
13	Photocatalytic titania coatings. Current Applied Physics, 2004, 4, 189-192.	2.4	71
14	Properties of nitrogen implanted and electron beam annealed bulk ZnO. Journal of Applied Physics, 2010, 107, .	2.5	70
15	Long–range transport of soil dust and smoke pollution in the South Asian region. Atmospheric Pollution Research, 2011, 2, 151-157.	3.8	70
16	Effect of annealing on the structural, electrical and magnetic properties of Gd-implanted ZnO thin films. Journal of Materials Science, 2012, 47, 1119-1126.	3.7	69
17	Fabrication of surface magnetic nanoclusters using low energy ion implantation and electron beam annealing. Nanotechnology, 2011, 22, 115602.	2.6	67
18	Raman scattering investigation of hydrogen and nitrogen ion implanted ZnO thin films. Current Applied Physics, 2008, 8, 291-294.	2.4	66

#	Article	IF	CITATIONS
19	Group-IV and V ion implantation into nanomaterials and elemental analysis on the nanometre scale. International Journal of Nanotechnology, 2009, 6, 369.	0.2	66
20	Morphology and characterization of TiO2 nanoparticles synthesized by arc discharge. Chemical Physics Letters, 2012, 521, 86-90.	2.6	66
21	Ion Beam Analysis of Amorphous and Nanocrystalline Group III-V Nitride and ZnO Thin Films. Journal of Electronic Materials, 2007, 36, 472-482.	2.2	63
22	Modification of electrical conductivity in RF magnetron sputtered ZnO films by low-energy hydrogen ion implantation. Current Applied Physics, 2006, 6, 495-498.	2.4	62
23	Preparation of SiO2 films with embedded Si nanocrystals by reactive r.f. magnetron sputtering. Thin Solid Films, 1998, 330, 202-205.	1.8	61
24	Carbonaceous aerosols in an urban tunnel. Atmospheric Environment, 2011, 45, 4463-4469.	4.1	61
25	Preliminary study of the sources of ambient air pollution in Serpong, Indonesia. Atmospheric Pollution Research, 2011, 2, 190-196.	3.8	55
26	Large room temperature magnetoresistance in ion beam synthesized surface Fe nanoclusters on SiO2. Applied Physics Letters, 2011, 98, .	3.3	55
27	Modulation of Field Emission Properties of ZnO Nanorods During Arc Discharge. Journal of Nanoscience and Nanotechnology, 2010, 10, 8239-8243.	0.9	53
28	lon-assisted deposition of amorphous GaN: Raman and optical properties. Applied Physics Letters, 2001, 78, 619-621.	3.3	49
29	Organic and Black Carbon in PM2.5 at an Urban Site at Dhaka, Bangladesh. Aerosol and Air Quality Research, 2012, 12, 1062-1072.	2.1	48
30	Field emission properties of self-assembled silicon nanostructures on n- and p-type silicon. Applied Physics Letters, 2004, 85, 3277-3279.	3.3	47
31	Flux pinning by discontinuous columnar defects in 74MeV Ag-irradiated YBa2Cu3O7 coated conductors. Physica C: Superconductivity and Its Applications, 2009, 469, 2060-2067.	1.2	46
32	Nonâ€diadromous recruitment in coastal populations of common bully (Gobiomorphus cotidianus). New Zealand Journal of Marine and Freshwater Research, 2003, 37, 301-313.	2.0	42
33	Nanostructuring of silicon (100) using electron beam rapid thermal annealing. Journal of Applied Physics, 2004, 96, 605-609.	2.5	40
34	The formation of narrow nanocluster bands in Ge-implanted SiO2-layers. Solid-State Electronics, 1999, 43, 1159-1163.	1.4	39
35	Identification of Particulate Matter Sources on an Hourly Time-Scale in a Wood Burning Community. Environmental Science & Technology, 2012, 46, 4767-4774.	10.0	39
36	Effect of Substrate Hardness on Splat Morphology in High-Velocity Thermal Spray Coatings. Journal of Thermal Spray Technology, 2006, 15, 663-669.	3.1	37

#	Article	IF	CITATIONS
37	Microstructural investigation of ion beam synthesised germanium nanoclusters embedded in SiO2 layers. Nuclear Instruments & Methods in Physics Research B, 1998, 142, 338-348.	1.4	33
38	AIR PARTICULATE RESEARCH CAPABILITY AT THE NEW ZEALAND ION BEAM ANALYSIS FACILITY USING PIXE AND IBA TECHNIQUES. International Journal of PIXE, 2005, 15, 249-255.	0.4	33
39	Quantitative study of molecularN2trapped in disordered GaN:O films. Physical Review B, 2004, 70, .	3.2	32
40	Magnetic and optical properties of the InCrN system. Journal of Applied Physics, 2005, 98, 043903.	2.5	32
41	Ion beam analysis of ion-assisted deposited amorphous GaN. Nuclear Instruments & Methods in Physics Research B, 2002, 190, 620-624.	1.4	29
42	26Al tracer diffusion in titanium doped single crystalline α-Al2O3. Solid State Ionics, 2008, 179, 373-379.	2.7	29
43	Hydrogen-related excitons and their excited-state transitions in ZnO. Physical Review B, 2017, 95, .	3.2	29
44	Hydrogen profiles of thin PVD silicon nitride films using elastic recoil detection analysis. Nuclear Instruments & Methods in Physics Research B, 1992, 68, 218-222.	1.4	28
45	Chemical bonding and interface analysis of ultrathin silicon-nitride layers produced by ion implantation and Electron Beam Rapid Thermal Annealing (EB-RTA). Applied Physics A: Solids and Surfaces, 1994, 59, 435-439.	1.4	28
46	Homogeneously size distributed Ge nanoclusters embedded in SiO2 layers produced by ion beam synthesis. Nuclear Instruments & Methods in Physics Research B, 1999, 147, 361-366.	1.4	28
47	Investigations of ultrathin silicon nitride layers produced by low-energy ion implantation and EB-RTA. Nuclear Instruments & Methods in Physics Research B, 1994, 89, 362-368.	1.4	26
48	Influence of environmental conditions on carbonaceous particle concentrations within New Zealand. Journal of Aerosol Science, 2010, 41, 134-142.	3.8	26
49	Composition and source contributions of air particulate matter pollution in a New Zealand suburban town. Atmospheric Pollution Research, 2012, 3, 143-147.	3.8	26
50	Change of surface structure of thin silicon nitride layers during electron beam rapid thermal annealing. Applied Physics Letters, 1994, 64, 2652-2654.	3.3	25
51	Nitrogen profiles of thin sputtered PVD silicon nitride films. Vacuum, 1993, 44, 367-370.	3.5	23
52	Formation of SiC-surface nanocrystals by ion implantation and electron beam rapid thermal annealing. Applied Physics Letters, 2005, 86, 013108.	3.3	23
53	Microstructural investigation of Sn nanoclusters in double-energy implanted and annealed SiO2 layers with cross-sectional TEM. Nuclear Instruments & Methods in Physics Research B, 1999, 152, 319-324.	1.4	22
54	Lithium and boron distributions in geological samples. Nuclear Instruments & Methods in Physics Research B, 1999, 158, 568-574.	1.4	22

#	Article	IF	CITATIONS
55	Role of oxides in high velocity thermal spray coatings. Nuclear Instruments & Methods in Physics Research B, 2002, 190, 518-523.	1.4	22
56	Evidence of Mechanical Interlocking of NiCr Particles Thermally Sprayed onto Al Substrates. Journal of Thermal Spray Technology, 2005, 14, 524-529.	3.1	21
57	Structural and magnetic properties of low-energy Gd implanted ZnO single crystals. Nuclear Instruments & Methods in Physics Research B, 2012, 272, 100-103.	1.4	21
58	Restrictions on fluorine depth profiling for exposure age dating in archaeological bones. Journal of Archaeological Science, 2008, 35, 535-552.	2.4	20
59	Oxygen and hydrogen profiles in metal surfaces following plasma immersion ion implantation of helium. Surface and Coatings Technology, 2001, 136, 217-222.	4.8	19
60	PIXE analysis of PM _{2.5} and PM _{2.5–10} for air quality assessment of Islamabad, Pakistan: Application of chemometrics for source identification. Journal of Environmental Science and Health - Part A Toxic/Hazardous Substances and Environmental Engineering, 2012, 47, 2016-2027.	1.7	19
61	Characterization of airborne particulate matter collected at Jakarta roadside of an arterial road. Journal of Radioanalytical and Nuclear Chemistry, 2013, 297, 165-169.	1.5	19
62	Carbonaceous aerosols in a wood burning community in rural New Zealand. Atmospheric Pollution Research, 2013, 4, 245-249.	3.8	19
63	Ultra-smooth diamond-like carbon coatings with high elasticity deposited at low temperature by direct ion beam deposition. Surface and Coatings Technology, 2014, 258, 956-962.	4.8	19
64	Universal characteristics of resonant-tunneling field emission from nanostructured surfaces. Journal of Applied Physics, 2007, 101, 123712.	2.5	18
65	Sources of particulate matter pollution in a small New Zealand city. Atmospheric Pollution Research, 2014, 5, 572-580.	3.8	18
66	Transition Metal Ion Implantation into Diamond-Like Carbon Coatings: Development of a Base Material for Gas Sensing Applications. Journal of Nanomaterials, 2015, 2015, 1-7.	2.7	18
67	Characterisation of 13C implantations in silicon by NRA [13C(p,?)14N] and RBS. Fresenius' Journal of Analytical Chemistry, 1995, 353, 483-486.	1.5	17
68	Low-energy 15N implantation in carbon for the synthesis of carbon nitride layers. Nuclear Instruments & Methods in Physics Research B, 1996, 113, 235-238.	1.4	17
69	Air quality study of Islamabad: preliminary results. Journal of Radioanalytical and Nuclear Chemistry, 2012, 293, 351-358.	1.5	17
70	A novel radial anode layer ion source for inner wall pipe coating and materials modification—Hydrogenated diamond-like carbon coatings from butane gas. Review of Scientific Instruments, 2014, 85, 085118.	1.3	17
71	28Si+ ion beams from Penning ion source based implanter systems for near-surface isotopic purification of silicon. Review of Scientific Instruments, 2018, 89, 123305.	1.3	17
72	Depth profile analysis: STEM-EDXvs. RBS. Surface and Interface Analysis, 1998, 26, 359-366.	1.8	16

5

#	Article	IF	CITATIONS
73	SiC nanoboulders on silicon – a nuclear reaction analysis study of low energy 13C implanted and subsequently electron beam annealed (100) silicon. Nuclear Instruments & Methods in Physics Research B, 2004, 217, 583-588.	1.4	16
74	Effect of crystal orientation on self-assembled silicon nanostructures formed by electron-beam annealing. Journal of Applied Physics, 2005, 97, 094301.	2.5	16
75	Synthesis of Zinc Oxide Nanorods and their Sensing Properties. Materials Science Forum, 0, 700, 150-153.	0.3	16
76	Reliable micro-measurement of strontium is the key to cracking the life-history code in the fish otolith. Nuclear Instruments & Methods in Physics Research B, 2000, 168, 109-116.	1.4	15
77	Ion beam analysis of nanoporous surfaces produced by He-implantation and oxidised by plasma-immersion ion-implantation. Nuclear Instruments & Methods in Physics Research B, 2000, 161-163, 1048-1053.	1.4	15
78	Characterisation of polycrystalline gallium nitride grown by plasma-assisted evaporation. Current Applied Physics, 2004, 4, 225-228.	2.4	15
79	Comparison of DC and RF Sputtered Zinc Oxide Films with Post-Annealing and Dry Etching and Effect on Crystal Composition. Japanese Journal of Applied Physics, 2005, 44, 7555-7560.	1.5	15
80	Low energy 15N and 14N implantation in chromium analysed by NRA and RBS. Nuclear Instruments & Methods in Physics Research B, 1993, 80-81, 459-462.	1.4	14
81	Atomic transport in metastable compounds: Case study of self-diffusion in < mml:math xmlns:mml="http://www.w3.org/1998/Math/MathML" display="inline"> < mml:mrow> < mml:mtext> Si < / mml:mtext> < mml:mo> â^3 < / mml:mo> < mml:mtext> C < / mml:mtext> using neutron reflectometry. Physical Review B. 2009, 80	<mml:mo< td=""><td>>a¹⁴</td></mml:mo<>	>a ¹⁴
82	Room temperature diamond-like carbon coatings produced by low energy ion implantation. Nuclear Instruments & Methods in Physics Research B, 2014, 331, 144-148.	1.4	14
83	Decorative black coatings on titanium surfaces based on hard bi-layered carbon coatings synthesized by carbon implantation. Surface and Coatings Technology, 2019, 358, 386-393.	4.8	14
84	Shallow Nanoporous Surface Layers Produced by Helium Ion Implantation. Advanced Materials, 2001, 13, 997-1000.	21.0	13
85	Particulate matter sources on an hourly timescale in a rural community during the winter. Journal of the Air and Waste Management Association, 2014, 64, 501-508.	1.9	13
86	Characterization of stoichiometric surface and buried SiN films fabricated by ion implantation using extended xâ€ray absorption fine structure. Journal of Applied Physics, 1996, 80, 2720-2727.	2.5	12
87	Strong Blue and Violet Photo- and Electroluminescence from Ge- and Si-Implanted Silicon Dioxide. Physica Status Solidi A, 1998, 165, 31-35.	1.7	12
88	Single phase nanocrystalline GaMnN thin films with high Mn content. Journal of Applied Physics, 2006, 100, 084310.	2.5	12
89	PIXE analysis of sand and soil from Ulaanbaatar and Karakurum, Mongolia. Nuclear Instruments & Methods in Physics Research B, 2008, 266, 4010-4019.	1.4	12
90	Sources and transport of particulate matter on an hourly time-scale during the winter in a New Zealand urban valley. Urban Climate, 2014, 10, 644-655.	5.7	12

#	Article	IF	CITATIONS
91	Characterisation of thin sputtered silicon nitride films by NRA, ERDA, RBS and SEM. Fresenius' Journal of Analytical Chemistry, 1993, 346, 177-180.	1.5	11
92	Ion beam analysis of light elements in nanoporous surfaces produced by single- and multiple-energy helium ion implantation. Nuclear Instruments & Methods in Physics Research B, 2002, 190, 718-722.	1.4	11
93	Optical conductivity and x-ray absorption and emission study of the band structure of MnN films. Physical Review B, 2005, 72, .	3.2	11
94	Field emission properties of self-assembled silicon nanostructures formed by electron beam annealing. Current Applied Physics, 2006, 6, 503-506.	2.4	11
95	Simultaneous formation of SiC and Si nanostructures on silicon by local ion implantation and electron beam annealing. Applied Physics Letters, 2006, 89, 153122.	3.3	11
96	Evolution of the structure and magneto-optical properties of ion beam synthesized iron nanoclusters. Journal of Materials Science, 2012, 47, 1127-1134.	3.7	11
97	High Energy Radial Deposition of Diamond-Like Carbon Coatings. Coatings, 2015, 5, 326-337.	2.6	11
98	Ferromagnetic order in diamond-like carbon films by Co implantation. Journal Physics D: Applied Physics, 2016, 49, 055002.	2.8	11
99	Height control of silicon nano-whiskers embedded in ultra thin silicon nitride layers by rapid thermal annealing. Physica E: Low-Dimensional Systems and Nanostructures, 2001, 11, 110-113.	2.7	10
100	Formation of micrometer sized crater shaped pits in silicon by low-energy 22Ne+ implantation and electron beam annealing. Nuclear Instruments & Methods in Physics Research B, 2003, 206, 179-183.	1.4	10
101	Self-assembly of magnetic nanoclusters in diamond-like carbon by diffusion processes enhanced by collision cascades. Applied Physics Letters, 2017, 110, .	3.3	10
102	Optical and compositional studies of SiN thin films with conventional and synchrotron radiation ellipsometry. Journal of Applied Physics, 1993, 73, 8514-8518.	2.5	9
103	Surface-near analyses of ultra thin silicon nitride layers by NRA, channeling RBS, FT IR ellipsometry and AFM. Fresenius' Journal of Analytical Chemistry, 1995, 353, 734-739.	1.5	9
104	Atmospheric pressure operation of a field emission diode based on self-assembled silicon nanostructures. Journal of Vacuum Science & Technology an Official Journal of the American Vacuum Society B, Microelectronics Processing and Phenomena, 2005, 23, 1445.	1.6	9
105	Formation of large SiC nanocrystals on Si(100) by 12C implantation and electron beam annealing. Current Applied Physics, 2006, 6, 507-510.	2.4	9
106	The strontium content of roe collected from spawning brown trout Salmo trutta L. reflects recent otolith microchemistry. Journal of Fish Biology, 2008, 72, 1847-1854.	1.6	9
107	Characterization of the Structural and Electrical Properties of Ion Beam Sputtered ZnO Films. Materials Science Forum, 2011, 700, 49-52.	0.3	9
108	Atomic retention and near infrared photoluminescence from PbSe nanocrystals fabricated by sequential ion implantation and electron beam annealing. Nuclear Instruments & Methods in Physics Research B, 2013, 307, 154-157.	1.4	9

#	Article	IF	CITATIONS
109	Improved current–voltage characteristics of downstream plasma enhanced chemical vapor deposition SiNx deposited at low temperature by using He as a dilution gas. Journal of Vacuum Science and Technology A: Vacuum, Surfaces and Films, 1997, 15, 1864-1873.	2.1	8
110	TRACE ELEMENT ANALYSIS OF SOUTH INDIAN GALLSTONES BY PIXE. International Journal of PIXE, 2002, 12, 137-144.	0.4	8
111	Patterned growth of self-assembled silicon nanostructures by ion implantation and electron beam annealing. Journal of Vacuum Science & Technology an Official Journal of the American Vacuum Society B, Microelectronics Processing and Phenomena, 2005, 23, 1459.	1.6	8
112	Ion beam analysis of rare earth nitride thin films. Nuclear Instruments & Methods in Physics Research B, 2008, 266, 1558-1561.	1.4	8
113	Synthesis and structure of Na+-intercalated WO3(4,4′-bipyridyl)0.5. Chemical Communications, 2010, 46, 4261.	4.1	8
114	Characterization of SiN thin films with spectroscopic ellipsometry. Physica B: Condensed Matter, 1993, 185, 342-347.	2.7	7
115	Layer and interface analysis of ultra thin ion beam produced silicon nitride layers by NRA and TEM. Nuclear Instruments & Methods in Physics Research B, 1996, 112, 284-288.	1.4	7
116	EFFECT OF ION-ENERGY ON THE PROPERTIES OF AMORPHOUS GaN FILMS PRODUCED BY ION-ASSISTED DEPOSITION. Modern Physics Letters B, 2001, 15, 1355-1360.	1.9	7
117	Sub-micron channeling contrast microscopy on reactive ion etched deep Si microstructures. Nuclear Instruments & Methods in Physics Research B, 2002, 190, 339-344.	1.4	7
118	Uptake of light elements of nanoporous layers formed by helium ion implantation. Nuclear Instruments & Methods in Physics Research B, 2003, 206, 1056-1061.	1.4	7
119	Enhanced Flux Pinning in MOD Second Generation HTS Wires by Silver- and Copper-Ion Irradiation. IEEE Transactions on Applied Superconductivity, 2007, 17, 3306-3309.	1.7	7
120	Self-assembled germanium nanostructures formed using electron-beam annealing. Current Applied Physics, 2008, 8, 276-279.	2.4	7
121	The Effect of Substrate Surface Oxides on the Bonding of NiCr Alloy Particles HVAF Thermally Sprayed onto Aluminum Substrates. Journal of Thermal Spray Technology, 2010, 19, 1024-1031.	3.1	7
122	SEM/EDS study of metal-assisted oxide desorption. Surface Science, 2010, 604, 1531-1535.	1.9	7
123	Correlation between microstructural and magnetic properties of Tb implanted ZnO. AIP Conference Proceedings, 2013, , .	0.4	7
124	Near-surface hydrogen depletion of diamond-like carbon films produced by direct ion deposition. Nuclear Instruments & Methods in Physics Research B, 2016, 371, 230-234.	1.4	7
125	Collision cascades enhanced hydrogen redistribution in cobalt implanted hydrogenated diamond-like carbon films. Nuclear Instruments & Methods in Physics Research B, 2017, 394, 6-11.	1.4	7
126	Light element detection in heavy matrices by high energy backscattering spectroscopy. Nuclear Instruments & Methods in Physics Research B, 1997, 122, 685-688.	1.4	6

#	Article	IF	CITATIONS
127	Characterization of the interdiffusion in Au-Al layers by RBS. Fresenius' Journal of Analytical Chemistry, 1997, 358, 59-63.	1.5	6
128	Nitrogen depth distribution, interface and structure analysis of SiNx layers produced by low-energy ion implantation. Mikrochimica Acta, 1997, 125, 337-341.	5.0	6
129	Investigation of the atomic interdiffusion and phase formation in ion beam-irradiated thin Cu-Al and Ag-Al multilayers byin situ RBS and XRD. Surface and Interface Analysis, 1998, 26, 160-174.	1.8	6
130	Twenty years of proton microprobe research in biominerals:. Nuclear Instruments & Methods in Physics Research B, 1999, 158, 1-5.	1.4	6
131	Helium ion implantation in SiAlON: Characterisation of cavity structures using TEM and IBA. Nuclear Instruments & Methods in Physics Research B, 2000, 166-167, 121-127.	1.4	6
132	Nitridation of Silicon Oxide Layers Studied with Ion Beam Analysis on the Nanometer Scale. Advanced Materials, 2001, 13, 1027-1030.	21.0	6
133	Co2MnX (XSi, Ge, Sn, SbSn) thin films grown by pulsed-laser deposition. Journal of Crystal Growth, 2005, 275, e1183-e1188.	1.5	6
134	Polycrystalline InGaN grown by MBE on fused silica glass. Physica Status Solidi C: Current Topics in Solid State Physics, 2005, 2, 2236-2239.	0.8	6
135	Nanostructuring at the surface of low-energy lead-implanted silicon by electron beam annealing. Surface and Interface Analysis, 2008, 40, 931-934.	1.8	6
136	Conductive atomic force microscopy study of self-assembled silicon nanostructures. Journal of Vacuum Science & Technology B, 2009, 27, 3051.	1.3	6
137	Controlled fabrication of Si nanostructures by high vacuum electron beam annealing. Physica E: Low-Dimensional Systems and Nanostructures, 2009, 41, 1853-1858.	2.7	6
138	Growth temperature and plasma power effects on N incorporation in InSbN grown by molecular beam epitaxy. Physica Status Solidi - Rapid Research Letters, 2009, 3, 263-265.	2.4	6
139	Nitrogen self-diffusion in magnetron sputtered Si-C-N films. Journal of Applied Physics, 2011, 109, 093522.	2.5	6
140	AIR PARTICULATE MATTER POLLUTION IN ULAANBAATAR CITY, MONGOLIA. International Journal of PIXE, 2012, 22, 165-171.	0.4	6
141	High temperature annealing effects on low energy iron implanted SiO2. Nuclear Instruments & Methods in Physics Research B, 2012, 273, 182-185.	1.4	6
142	Formation of nanoclusters with varying Pb/Se concentration and distribution after sequential Pb+ and Se+ ion implantation into SiO2. Nuclear Instruments & Methods in Physics Research B, 2012, 273, 199-202.	1.4	6
143	Long term airborne lead pollution monitoring in Bandung, Indonesia. International Journal of PIXE, 2014, 24, 151-159.	0.4	6
144	Observation of multiple magnetic phases and complex nanostructures in Co implanted amorphous carbon films. Journal of Physics and Chemistry of Solids, 2019, 127, 158-163.	4.0	6

#	Article	IF	CITATIONS
145	Combined NRA, channeling-RBS and FTIR ellipsometry analyses for the determination of the interface and bonding state of thin SiOx and SiNxOy layers. Fresenius' Journal of Analytical Chemistry, 1995, 353, 403-407.	1.5	5
146	Investigation of ultra thin SiNxOy layers produced by low-energy ion implantation with NRA and channeling-RBS. Nuclear Instruments & Methods in Physics Research B, 1996, 108, 62-64.	1.4	5
147	Depth profile analysis and study of the electronic properties of silicon nitride layers produced by ion implantation. Nuclear Instruments & Methods in Physics Research B, 1996, 113, 223-226.	1.4	5
148	Surface and layer state of thin Au-Al layers after high-energy ion irradiation measured by RBS, scanning ion microprobe and SEM. Surface and Interface Analysis, 1997, 25, 889-895.	1.8	5
149	Depth profiling: RBS versus energy-dispersive X-ray imaging using scanning transmission electron microscopy. Nuclear Instruments & Methods in Physics Research B, 2000, 161-163, 221-226.	1.4	5
150	HEAVY METAL POLLUTION STUDIES OF SUSPENDED SEDIMENTS IN WAIWHETU STREAM WATER BY PIXE. International Journal of PIXE, 2002, 12, 189-197.	0.4	5
151	Surface structuring and phase formation in thin metallic layers deposited at various temperatures. Surface and Interface Analysis, 2002, 33, 1-6.	1.8	5
152	Microprobe analysis of light elements in nanoporous surfaces produced by helium ion implantation. Nuclear Instruments & Methods in Physics Research B, 2003, 210, 543-547.	1.4	5
153	GROWTH OF SIC NANOSTRUCTURES ON SI (100) USING LOW ENERGY CARBON ION IMPLANTATION AND ELECTRON BEAM RAPID THERMAL ANNEALING. International Journal of Nanoscience, 2004, 03, 425-430.	0.7	5
154	CHRONOSEQUENCES OF STRONTIUM IN THE OTOLITHS OF TWO NEW ZEALAND MIGRATORY FRESHWATER FISH, INANGA (GALAXIAS MACULATUS) AND KOARO (G. BREVIPINNIS). International Journal of PIXE, 2005, 15, 95-101.	0.4	5
155	CHARACTERIZATION OF ZnO FILMS BY ION BEAM ANALYSIS. International Journal of Modern Physics B, 2006, 20, 4655-4660.	2.0	5
156	Surface cavities produced by high-dose nitrogen ion implantation into silicon. Surface and Interface Analysis, 2007, 39, 698-701.	1.8	5
157	Oxygen uptake of InN thin films as determined by ion beam analysis. Thin Solid Films, 2007, 515, 3736-3739.	1.8	5
158	Sub-surface retention of Pb atoms in silicon after low-energy ion implantation and electron beam annealing. Nuclear Instruments & Methods in Physics Research B, 2008, 266, 1553-1557.	1.4	5
159	PIXE ANALYSIS OF SEDIMENTS AFFECTED BY THE DECEMBER 2004 INDIAN OCEAN TSUNAMI. International Journal of PIXE, 2008, 18, 227-240.	0.4	5
160	RECENT DEVELOPMENTS IN THE AIR PARTICULATE RESEARCH CAPABILITY AT THE NEW ZEALAND ION BEAM ANALYSIS FACILITY. International Journal of PIXE, 2012, 22, 121-130.	0.4	5
161	Size-fractionated airborne particulate matter characterization of a residential area near Islamabad airport by IBA methods. Journal of Radioanalytical and Nuclear Chemistry, 2012, 293, 279-287.	1.5	5
162	Depth Profiling by Ion Beams Analysis Techniques for the Characterization of Interdiffusion in Multilayered Au-Al Systems. Surface and Interface Analysis, 1996, 24, 868-874.	1.8	4

#	Article	IF	CITATIONS
163	NUCLEAR MICROPROBE AND RAMAN INVESTIGATION OF THE CHEMISTRY OF THE SHELL OF THE PACIFIC OYSTER, CRASSOSTREA GIGAS. International Journal of PIXE, 1999, 09, 345-352.	0.4	4
164	USE OF IBA TECHNIQUES TO CHARACTERIZE HIGH VELOCITY THERMAL SPRAY COATINGS. Modern Physics Letters B, 2001, 15, 1428-1436.	1.9	4
165	Structural and optical properties of indium nitride grown by plasma-assisted molecular beam epitaxy. , 2004, , .		4
166	A method for improving the efficiency of proton microprobe profiling of strontium in otoliths using a vacuum compatible Nal detector. Nuclear Instruments & Methods in Physics Research B, 2004, 217, 521-524.	1.4	4
167	Depth profiling of light elements in PAMBE-grown GaN and helium-implanted titanium with heavy ion time-of-flight elastic recoil detection. Surface and Interface Analysis, 2004, 36, 317-322.	1.8	4
168	Carbon depth profiling of superconducting YBCO thin films on nanometer scale. Current Applied Physics, 2004, 4, 292-295.	2.4	4
169	Heavy-ion elastic recoil detection analysis as a useful tool for tracking experimental modifications in bulk calcium silicates. Surface and Interface Analysis, 2005, 37, 695-698.	1.8	4
170	ELEMENTAL ANALYSIS AND SOURCE APPORTIONMENT OF AMBIENT PARTICULATE MATTER AT MASTERTON, NEW ZEALAND. International Journal of PIXE, 2005, 15, 225-231.	0.4	4
171	Elemental analysis of urban stormwater particulate matter by PIXE. Nuclear Instruments & Methods in Physics Research B, 2007, 258, 435-439.	1.4	4
172	Microprobe analysis of brine shrimp grown on meteorite extracts. Nuclear Instruments & Methods in Physics Research B, 2007, 260, 184-189.	1.4	4
173	Diffusion of Pb in carbon ion-implanted silicon: Discovery of a new crystalline phase after electron beam annealing. Vacuum, 2008, 82, 1306-1311.	3.5	4
174	Fluxâ€Pinning Centers In Metalâ€Organic Deposited YBCO Coated Conductors. AIP Conference Proceedings, 2009, , .	0.4	4
175	Compositional and Structural Study of Gd Implanted ZnO Films. , 2009, , .		4
176	Onset Temperature for Si Nanostructure Growth on Si Substrate During High Vacuum Electron Beam Annealing. Journal of Nanoscience and Nanotechnology, 2009, 9, 2950-2955.	0.9	4
177	Electron Beam Annealing of Fe+ Implanted Si Nanostructures. Journal of Nanoscience and Nanotechnology, 2010, 10, 6556-6561.	0.9	4
178	Multiblock analysis of environmental measurements: A case study of using Proton Induced X-ray Emission and meteorology dataset obtained from Islamabad Pakistan. Chemometrics and Intelligent Laboratory Systems, 2011, 107, 31-43.	3.5	4
179	Determination of chemical elements in airborne particulate matter collected at Lembang, Indonesia by particle induced X-ray emission. Journal of Radioanalytical and Nuclear Chemistry, 2013, 297, 177-182.	1.5	4
180	Loss of implanted heavy elements during annealing of ultra-shallow ion-implanted silicon: The complete picture. Applied Surface Science, 2014, 314, 322-330.	6.1	4

#	Article	IF	CITATIONS
181	Structural and chemical changes during the growth of Fe nanoparticles in SiO _{2 under low energy ion implantation. International Journal of Nanotechnology, 2014, 11, 466.}	0.2	4
182	The effect of hydrogen and temperature on the optical gaps of silicon nitride and comparative stoichiometry studies on SiN thin films. Journal of Non-Crystalline Solids, 1995, 187, 291-296.	3.1	3
183	Microstructural characterization of stoichiometric buried Si3N4 films. Nuclear Instruments & Methods in Physics Research B, 1996, 113, 227-230.	1.4	3
184	Study of electronic properties and depth profiles of buried and near-surface silicon nitride layers produced by ion implantation. Nuclear Instruments & Methods in Physics Research B, 1997, 124, 506-514.	1.4	3
185	Light element impurities in ion beam bombarded Auî—,Al layers. Nuclear Instruments & Methods in Physics Research B, 1998, 136-138, 516-520.	1.4	3
186	Phase formation in ion beam bombarded Al-Au multilayers using high-current 2.0 MeV4He+ ions. Surface and Interface Analysis, 1998, 26, 650-658.	1.8	3
187	Compositional and structural studies of amorphous GaN grown by ion-assisted deposition. Materials Research Society Symposia Proceedings, 2001, 693, 579.	0.1	3
188	lon microscope investigations of non-uniform surfaces of thin SiO2 films produced by high-temperature nitridation experiments. Nuclear Instruments & Methods in Physics Research B, 2001, 181, 354-359.	1.4	3
189	CHARACTERIZATION OF SUPERCONDUCTING MULTILAYERED FILMS USING RBS AND TEM. Modern Physics Letters B, 2001, 15, 1314-1320.	1.9	3
190	FLUORINE AND CALCIUM PROFILING BY PIGE/PIXE FOR EXPOSURE AGE DATING IN ARCHAEOLOGY. International Journal of PIXE, 2005, 15, 327-335.	0.4	3
191	A nuclear reaction analysis and optical microscopy study on controlled growth of large SiC nanocrystals on Si formed by low-energy ion implantation and electron beam annealing. Nuclear Instruments & Methods in Physics Research B, 2006, 249, 105-108.	1.4	3
192	Characteristics of hetero-junction diodes based on ion beam sputtered ZnO thin films. , 2007, , .		3
193	Field emission measured from nanostructured germanium and silicon thin films. Applied Surface Science, 2009, 256, 1003-1005.	6.1	3
194	Sensors based on metal oxide nanostructures synthesized by arc discharge. , 2011, , .		3
195	High conductivity transparent carbon nanotube films deposited from superacid. Nanotechnology, 2011, 22, 309502.	2.6	3
196	Room temperature oxidation of magnetron sputtered Si–C–N films. Applied Surface Science, 2012, 258, 2944-2947.	6.1	3
197	Use of micro-proton elastic scattering analysis to determine water content in geological powders. Nuclear Instruments & Methods in Physics Research B, 2013, 306, 257-260.	1.4	3
198	Positioning of cobalt atoms in amorphous carbon films by pre-selecting the hydrogen concentration. Nuclear Instruments & Methods in Physics Research B, 2017, 409, 116-120.	1.4	3

#	Article	IF	CITATIONS
199	Molecular carbon nitride ion beams for enhanced corrosion resistance of stainless steel. Nuclear Instruments & Methods in Physics Research B, 2017, 409, 86-90.	1.4	3
200	Influence of the Native Oxide Layer on the Silicon Surface During Initial Stages of Nitridation. Mikrochimica Acta, 2001, 137, 49-56.	5.0	2
201	PROBING FOR FLUORINE IN NITRIDED SIO2 FILMS BY ION BEAM ANALYSIS. Modern Physics Letters B, 2001, 15, 1332-1338.	1.9	2
202	CHARACTERISATION OF CONDUCTING POLYMERS USING ION BEAM ANALYSIS. Modern Physics Letters B, 2001, 15, 1411-1418.	1.9	2
203	PROBING FOR STRONTIUM PATTERNS IN OTOLITHS OF COMMON BULLIES FROM THE CLUTHA RIVER, NEW ZEALAND. International Journal of PIXE, 2002, 12, 109-115.	0.4	2
204	NEXAFS and AFM characterization of Si implanted GaN. Nuclear Instruments & Methods in Physics Research B, 2003, 200, 120-125.	1.4	2
205	AN OVERVIEW OF THE RCA/IAEA ACTIVITIES IN THE AUSTRALASIAN REGION USING NUCLEAR ANALYSIS TECHNIQUES FOR MONITORING AIR POLLUTION. International Journal of PIXE, 2005, 15, 271-276.	0.4	2
206	Atom ingress from synthetic body fluid into nanoporous layers formed in titanium by helium ion-implantation. Current Applied Physics, 2006, 6, 327-330.	2.4	2
207	Optical and compositional properties of indium nitride grown by plasma assisted molecular beam epitaxy. Smart Materials and Structures, 2006, 15, S87-S91.	3.5	2
208	Lowâ \in energy Fe+ ion implantation into silicon nanostructures. , 2009, , .		2
209	Diffusion of Pb in (100) Si under electron beam annealing following dual ion implantations of Pb/Ne, Pb/O and Pb/N. Vacuum, 2010, 84, 1103-1110.	3.5	2
210	Growth of silicon carbide surface nanocrystals on silicon under high-temperature vacuum annealing. Vacuum, 2011, 86, 165-170.	3.5	2
211	Effects of Implanted Fe ⁺ Fluences on the Growth and Magnetic Properties of Surface Nanoclusters. Materials Science Forum, 0, 700, 37-40.	0.3	2
212	Solid phase epitaxy of ultra-shallow Sn implanted Si observed using high-resolution Rutherford backscattering spectrometry. Applied Physics Letters, 2012, 101, 081602.	3.3	2
213	Enhanced reduction of silicon oxide thin films on silicon under electron beam annealing. Nuclear Instruments & Methods in Physics Research B, 2014, 332, 421-425.	1.4	2
214	Ferromagnetism in a diamond-like carbon film after nickel implantation. International Journal of Nanotechnology, 2017, 14, 100.	0.2	2
215	Molecular ion implantation in silicon. Mikrochimica Acta, 1997, 125, 313-316.	5.0	1
216	X-ray reflectivity investigation of near-surface density changes induced in Al–Au multilayers by high-current ion beam bombardment. Nuclear Instruments & Methods in Physics Research B, 1998, 143, 422-426.	1.4	1

#	Article	IF	CITATIONS
217	INFLUENCE OF OXYGEN IMPURITIES ON ION BEAM INDUCED INTERDIFFUSION IN THIN Au-Al MULTILAYERS DEPOSITED ON DIFFERENT SUBSTRATES. Modern Physics Letters B, 2001, 15, 1370-1381.	1.9	1
218	Probing for heavy element impurities in the shell of the Pacific oyster, Crassostrea gigas, with nuclear microscopy. Nuclear Instruments & Methods in Physics Research B, 2003, 210, 418-423.	1.4	1
219	SUPPRESSION OF SILICON NANOSTRUCTURE GROWTH BY MEDIUM ENERGY NITROGEN ION IMPLANTATION. International Journal of Nanoscience, 2004, 03, 431-437.	0.7	1
220	Analysis of heteroepitaxial germanium on gallium arsenide grown by pulsed laser deposition. Current Applied Physics, 2004, 4, 229-232.	2.4	1
221	Optimization of Non-Fluorine Sol-Gel Derived YBCO Thin Films. Journal of Electroceramics, 2004, 13, 361-365.	2.0	1
222	Plasma immersion nitrogen implantation into silicon and rapid thermal electron beam annealing for surface structuring. Current Applied Physics, 2004, 4, 241-244.	2.4	1
223	Characterisation of ZnO Thin Films Grown Directly on Sapphire by PAMBE. , 0, , .		1
224	EVIDENCE FOR GIANT KOKOPU MIGRATION BETWEEN FRESHWATER ENVIRONMENTS FROM MICROPIXE MEASUREMENTS OF SR IN OTOLITHS. International Journal of PIXE, 2005, 15, 139-145.	0.4	1
225	Field Eemission Resonances from Self-Aassembled Silicon Nnanostructures. , 2006, , .		1
226	X-ray diffraction study of low-energy carbon-ion implanted Si(001). Surface and Interface Analysis, 2007, 39, 415-418.	1.8	1
227	Deuteron microprobe analysis of carbon in the transition region between SiC and Si nanostructures grown on Si. Nuclear Instruments & Methods in Physics Research B, 2007, 260, 325-328.	1.4	1
228	THREE DIMENSIONAL IMAGING OF OTOLITHS. International Journal of PIXE, 2008, 18, 131-137.	0.4	1
229	Depth Profiling of N and C in Ion Implanted ZnO and Si Using Deuterium Induced Nuclear Reaction Analysis. , 2008, , .		1
230	Ordered array of self-assembled SiC nanocrystals fabricated by selective oxide desorption and nanosphere lithography. Nanotechnology, 2010, 21, 495302.	2.6	1
231	Dual N/Pb ion-implanted Si: Temperature dependence of the novel shift of the Pb peak under electron beam annealing. Applied Surface Science, 2011, 257, 4856-4862.	6.1	1
232	Ionâ€beam synthesis of 3Câ€SiC surface layers on silicon. Surface and Interface Analysis, 2012, 44, 399-404.	1.8	1
233	Arsenic and air pollution in New Zealand. Arsenic in the Environment Proceedings, 2014, , 394-395.	0.0	1
234	Ion Current Dependent Interdiffusion in Au-Al Layers during Ion Beam Irradiation. Defect and Diffusion Forum, 1997, 143-147, 1303-1310.	0.4	0

#	Article	IF	CITATIONS
235	UPTAKE OF LIGHT ELEMENTS IN THIN METALLIC FILMS. Modern Physics Letters B, 2001, 15, 1382-1390.	1.9	0
236	Demonstration of a new calibration standard for strontium measurements in otoliths based on high energy Sr ion implantation. Journal of Fish Biology, 2002, 61, 853-857.	1.6	0
237	Surface smoothing of thin HTc YBa2Cu3O7â^l´ superconducting films by high-energy iodine ions. Current Applied Physics, 2004, 4, 288-291.	2.4	0
238	Self-assembled silicon nanostructure growth by electron beam annealing. , 2004, , .		0
239	Field-Emission Diode and Triode Structures Using Self-Assembled Silicon Nanostructure Cathodes. , 2006, , .		Ο
240	Optimised process for fabricating functional silicon nanowhisker arrays. Current Applied Physics, 2008, 8, 395-399.	2.4	0
241	Field Emission from Silicon Implanted with Carbon and Nitrogen Followed by Electron Beam Annealing. Journal of Electronic Materials, 2010, 39, 1262-1267.	2.2	Ο
242	Fabrication and characterization of integrated field emission diodes using self-assembled-silicon-nanostructure cathodes. , 2010, , .		0
243	Microstructure Evolution in Nitrogen Implanted Sapphire. Advanced Materials Research, 0, 275, 222-225.	0.3	Ο
244	Magnetic-ion-doped silicon nanostructures fabricated by ion implantation and electron beam annealing. Nuclear Instruments & Methods in Physics Research B, 2013, 307, 131-136.	1.4	0
245	Transition metal doped metal oxide nanostructures synthesized by arc discharge method. , 2013, , .		Ο
246	Layer and interface analysis of ultra thin ion beam produced silicon nitride layers by NRA and TEM. , 1996, , 284-288.		0